Available online at www.sciencedirect.com

ScienceDirect

IFAC PapersOnLine 58-24 (2024) 287–290

Interfacing with Prototype Instrumented Smart Screwdriver for Bone Screw Torque Regulation

Jack Wilkie [*] **Georg Rauter** [**] **Knut Möller** [***]

[*] *Institute for Technical Medicine, Hochschule Furtwangen,*
Villingen-Schwenningen, Germany, (e-mail: wij@hs-furtwangen.de).
[**] *BIROMED-Lab, Department of Biomedical Egineering, University*
of Basel, Basel, Switzerland, (e-mail: georg.rauter@unibas.ch).
[***] *Institute for Technical Medicine, Hochschule Furtwangen,*
Villingen-Schwenningen, Germany, (e-mail: moe@hs-furtwangen.de).

Abstract: Bone screws are used in a variety of orthopaedic procedures for fracture or implant fixation. In these procedures, it is important not to over- or under-tighten the screws. Prior work has developed real-time models to optimise the tightening torque, however testing has been limited to bench-top test rigs. This paper investigates interfacing with a handheld smart screwdriver to perform testing under less controlled circumstances.

The smart screwdriver was mounted in a previously used test-rig and was used to insert a screw into a test sample. The torque and rotation signals from both the test rig and the screwdriver were recorded and compared.

There was general agreement between the signals from the test rig and the screwdriver. Notable deviations occurred due to more aggressive torque smoothing in the screwdriver, truncating low torques below 0.4 N·m to 0 N·m in the screwdriver, and saturation of the gyroscope in the screwdriver used for rotational measurement. It is anticipated that all of these can be addressed through simple software changes.

Keywords: smart screwdriver, comparison, bone screws, polyurethane foam, torque, angular displacement, rotation

1. INTRODUCTION

Bone screws are used in a variety of orthopaedic procedures for fracture (Fernandez, 1990) and implant (Kieser et al., 2018) fixation. During these procedures, the tightening torque used for the screw can impact the outcomes of the surgery. If too tight, the screw may damage the threads formed in the bone, causing a weaker fixation that may be more likely to fail under load or shock(Feroz Dinah et al., 2011). If too loose, the screw may back out over time, compromising the fixation stability, or leading to loose implants/debris and other further damage(Evans et al., 1990).

In current surgical practice, screws are generally tightened ad-hoc, with the surgeon using their intuition, experience, and tactile feedback to determine the appropriate tightness. While surgeons are skilled professionals and this works adequately in many cases, it is still a subjective judgment, and may be impacted by human factors like stress and fatigue, and less experienced or skilled surgeons may not achieve the same fixation quality as more skilled ones(Stoesz et al., 2014). Hence, an automated torque determination system my be useful in a traditional operating theater to ease the load on surgeons, and provide a more objective level of torquing. Additionally, with the advent of automated, semi-automated, or robot-assisted surgery, surgeons may no longer directly/physically control tightening operations, necessitating a computational method for torque-control.

Prior work on real-time optimal torque determination includes empirical models (Reynolds et al., 2017; Thomas et al., 2008; Wright et al., 2020) and a physically based model (Wilkie et al., 2021b,a). Focusing on the physically based model, previous work has developed models of the insertion phase for determining the material strength(Wilkie et al., 2021b), and the tightening phase for determining the torque limit based on the previously determined material strength(Wilkie et al., 2021a). These models have also been tested separately(Wilkie et al., 2021a,c) with some limited testing together(Wilkie et al., 2023). In all cases the models were tested on a custom-built test rig, which may not perfectly transfer to practical application on a smart screwdriver.

In this paper we evaluate a potential smart screwdriver prototype that will be used to test the optimal torque models described above. This will be compared against a bench-mounted test rig(Wilkie and Möller, 2021) that

---

⋆ The screwdriver was developed as part of the BMBF funded CoHMED Projects 12FH5K02IA and 12FH5E02IA.

Conflict of Interest: This work was performed in partial collaboration with Kammerer Medical Systems GmbH & Co KG, who may intend to bring a related product to market in the future.

Full funding info to add before final submission.

10.1016/j.ifacol.2024.11.051

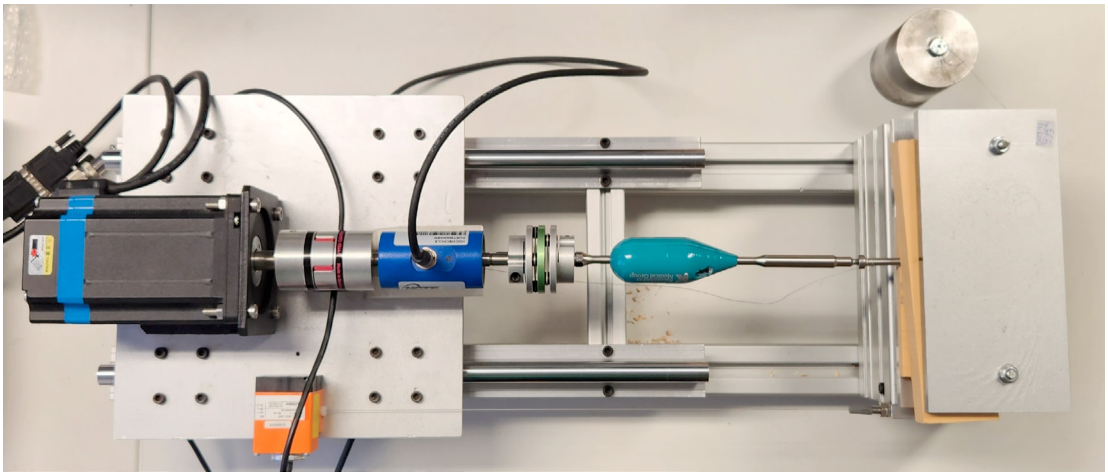

Fig. 1. Test rig setup used to evaluate smart screwdriver.

was previously used to test the models. Any deficiencies found will be reported so that they can be addressed before the screwdriver is used for testing the models. In this case the screwdriver is only used as-is, however software changes may be made in the future in consultation with the company that developed the prototype.

2. METHODS

2.1 Materials

A prototype smart screwdriver (Kammerer Medical Systems GmbH & Co KG) was acquired as part of a research cooperation agreement. This screwdriver contained a PCB with a Wi-Fi capable microcontroller, an MPU6050 gyroscope, and a strain-gauge based torque sensor connected to the screwdriver's shaft. The screwdriver connects to a hard-coded Wi-Fi network and provides an HTTP webserver to display the sensor outputs (torque, acceleration, rotation) and device status (battery level) in a web browser.

The screwdriver was compared against the readings from a previously developed screw-insertion test rig(Wilkie and Möller, 2021). This used a closed loop stepper motor (34HS46-6004D-E100, OMC Corp. Ltd.) to drive a screw into test blocks via a shaft that passed through a rotation torque sensor (NCTE-2300-05-1-AU-0-0, NCTE AG) that measures the torque and rotation of the screw. Additionally a draw-wire encoder (D5.2501.2421.1000, Fritz Kübler GmbH) on the test rig measures the linear motion of the screw and a counterweight on a pulley provides a constant axial force. This test rig outputs readings over a USB serial interface, where it can also receive commands to control the stepper motor for consistent powered screw insertion. A custom C# application was developed to interface with this rig and save data to a file. The software was designed to connect to multiple data sources simultaneously, and to be expandable to more types of devices (serial, USB, Bluetooth, Wi-Fi, etc.) in the future.

The prototype screwdriver was mounted in the screw insertion test rig between the torque sensor and the screw, as shown in Fig. 1. The results in the screwdriver shaft being exposed to the same torque values and rotation as the shaft travelling through the rotational torque sensor. A new device class was developed for the test rig interface software. The screwdriver used HTTP server-sent events (MIME type: text/event-stream) to send data to the web interface. The class was designed to open an TCP/HTTP connection requesting to receive events from the screwdriver, then parse the event messages as they were received. A simple custom parser was written, as server-sent events are generally processed by JavaScript and no C# package/library was found to do this without changing the screwdriver software.

2.2 Testing

A screw was found that fitted the end of the smart screwdriver, and was driven between two clamped blocks of rigid polyurethane foam to generate resistance torque. This setup was just to provide some resistance torque for comparative measurements, so the inconsistency in the exact values displayed on the torque plots is not important here.

The screw/screwdriver was driven with a triangular velocity profile to test the torque and rotation sensing abilities of the smart screwdriver prototype over a variety of speeds. The first test inserted the screw 20 turns over 60 seconds, ramping up to 240 degrees per second and down to zero. The second test halved the insertion time and ramped up to 480 degrees per second.

3. RESULTS

The torque readings from the first test in Fig. 2 from the screwdriver and the test rig are largely similar. The screwdriver currently has a hard-coded minimum torque of 0.4 N·m, below which the value output will be 0 N·m. Above this the readings are similar. Notably there is more fluctuation in the signal from the test rig torque sensor, likely due to the built-in smoothing in the screwdriver, while the test rig attempts to provide the full bandwidth available from its sensor (1000 Hz according to the datasheet).

The angular displacement readings from the first test are shown in Fig. 3a and angular velocity in Fig. 3b. For the most part these are similar, however the screwdriver

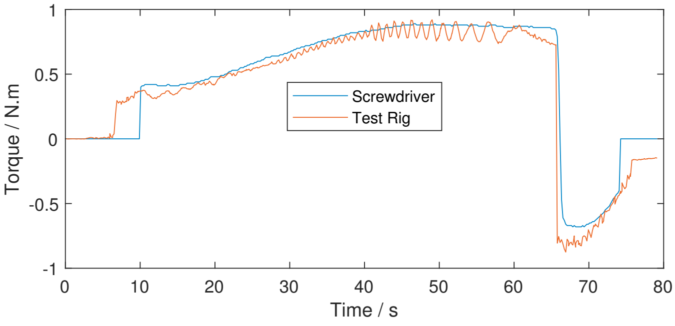

(a) First (lower speed) test.

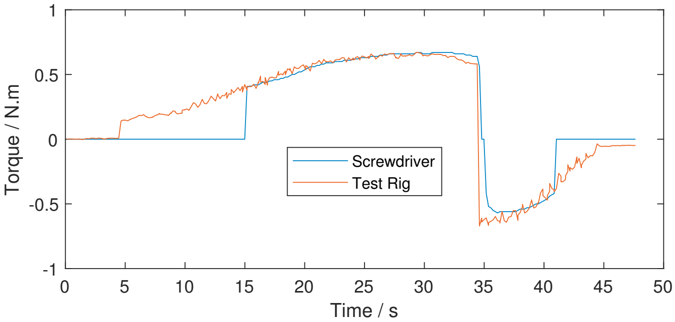

(b) Second (higher speed) test.

Fig. 2. Torque signals from screwdriver and test rig.

appears to over-read the angular velocity and integrates this to give a larger maximum angular displacement. As the test rig uses a quadrature encoder, its angular displacement reading is considered to be more accurate/definitive. The saturation of the screwdriver gyroscope reading is also visible, and it truncates the angular velocity reading at 260 deg·s^{-1}. This is even clearer in the angular displacement and velocity results from the second test shown in Fig. 4a and Fig. 4b, where the screwdriver clearly misreads the velocity at higher speeds, giving a measured trapezoidal velocity profile instead of triangular. This is also visible as a straight section of the angular displacement plot where it should be curved.

4. DISCUSSION

In general the sensors in the smart screwdriver were found to be reasonably accurate when compared to a fixed torque/rotation sensor. However the gyroscope for rotational measurement would require further calibration/characterisation for better accuracy (possibly a more accurate model can be used if required), and a larger range of angular velocity measurement is likely necessary, although this is possible via a configuration option with the MPU-6050 sensor currently utilised according to the data-sheet, allowing measurements up to 2000 deg·s^{-1}.

There are also some peaks in the velocity plots from the screwdriver due to the numeric differentiation used in the data processing, some are filtered out, however to avoid excessively smoothing the data we avoided using an excessively strong low-pass filter. As the gyroscope sensor does measure angular velocity directly, the firmware could be modified to send this as well as the integrated position.

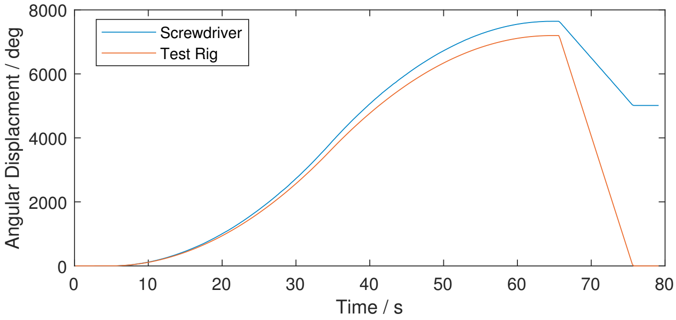

(a) Angular displacement.

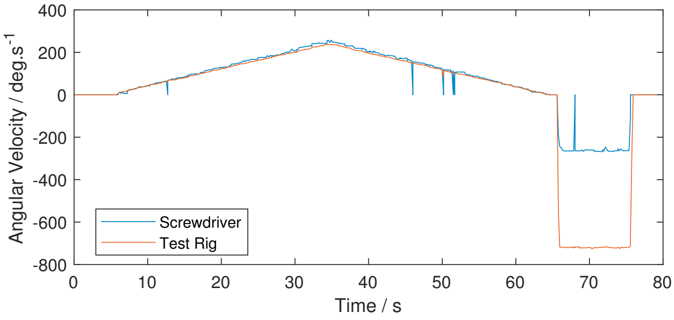

(b) Angular velocity.

Fig. 3. Angular displacement and angular velocity signals from screwdriver and test rig for first (lower speed) test.

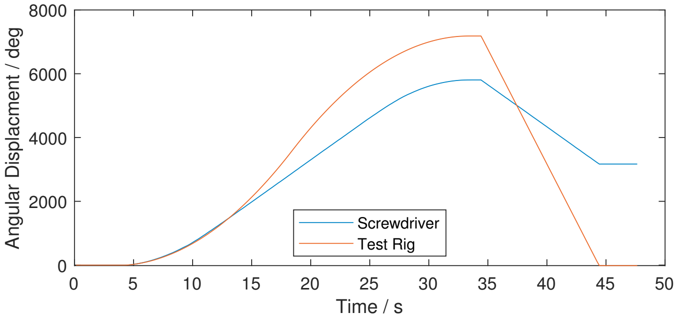

(a) Angular displacement.

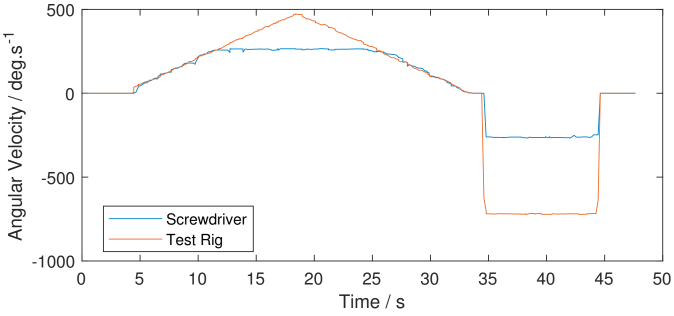

(b) Angular velocity.

Fig. 4. Angular displacement and angular velocity signals from screwdriver and test rig for second (higher speed) test.

The torque sampling rate was relatively low compared to the test rig, this is defined with a period of 180 ms in the firmware, however it is unclear if this rate was selected as a limitation of the hardware used; higher rates should be tested to see if they affect the firmware stability. It appears that some smoothing is performed; after examining the code, this appears to be software based, so an increased torque measurement bandwidth may be easily achieved through software changes if it is not also limited by the hardware (e.g. with analog low-pass filters).

In general further understanding of the screwdriver prototype and some minor changes to the software will likely yield significantly improved performance. After these changes, the screwdriver can be testing with currently developed torque-limit-regulation models to prove the applicability of them in the context of a handheld screwdriver. However, we must first discuss with the company to get permission to test these firmware changes.

5. CONCLUSION

A prototype smart bone screwdriver was compared with a bone screw insertion test rig to characterize the torque and angular displacement signals from it.

Reasonable agreement for both signals were found, with some caveats. The torque signal jumps to 0 N·m when below 0.4 N·m applied, and is possibly smoothed excessively. The angular position signal is subject to gyroscope drift, due to slight miss-calibrations of the low-cost gyroscope currently used, and the relatively low speed for angular velocity saturation given the current configuration.

Some minor software changes to the smart screwdriver may significantly improve the performance of the screwdriver, prior to using it for verification of torque limit determination models in a handheld context, or a future iteration may be used to clinically test automated torque-regulation.

ACKNOWLEDGEMENTS

REFERENCES

Evans, M., Spencer, M., Wang, Q., White, S.H., and Cunningham, J.L. (1990). Design and testing of external fixator bone screws. *Journal of Biomedical Engineering*, 12(6), 457–462. doi:10.1016/0141-5425(90)90054-Q.

Fernandez, D.L. (1990). Anterior bone grafting and conventional lag screw fixation to treat scaphoid nonunions. *The Journal of Hand Surgery*, 15(1), 140–147. doi:10.1016/S0363-5023(09)91122-4.

Feroz Dinah, A., Mears, S.C., Knight, T.A., Soin, S.P., Campbell, J.T., and Belkoff, S.M. (2011). Inadvertent Screw Stripping During Ankle Fracture Fixation in Elderly Bone. *Geriatr Orthop Surg Rehabil*, 2(3), 86–89. doi:10.1177/2151458511401352.

Kieser, D.C., Ailabouni, R., Kieser, S.C., Wyatt, M.C., Armour, P.C., Coates, M.H., and Hooper, G.J. (2018). The use of an Ossis custom 3D-printed tri-flanged acetabular implant for major bone loss: Minimum 2-year follow-up. *HIP International*, 28(6), 668–674.

Reynolds, K.J., Mohtar, A.A., Cleek, T.M., Ryan, M.K., and Hearn, T.C. (2017). Automated Bone Screw Tightening to Adaptive Levels of Stripping Torque. *Journal of Orthopaedic Trauma*, 31(6), 321–325. doi:10.1097/BOT.0000000000000824.

Stoesz, M.J., Gustafson, P.A., Patel, B.V., Jastifer, J.R., and Chess, J.L. (2014). Surgeon Perception of Cancellous Screw Fixation. *Journal of Orthopaedic Trauma*, 28(1), e1. doi:10.1097/BOT.0b013e31829ef63b.

Thomas, R.L., Bouazza-Marouf, K., and Taylor, G.J.S. (2008). Automated surgical screwdriver: Automated screw placement. *Proc Inst Mech Eng H*, 222(5), 817–827. doi:10.1243/09544119JEIM375.

Wilkie, J.A. and Möller, K. (2021). Test rig for bone screw insertion modelling. In *15th Interdisciplinary Symposium Automation in Medical Engineering (AUTOMED)*, 2. Basel, Switzerland. doi:10.5281/zenodo.4922937.

Wilkie, J., Docherty, P.D., and Möller, K. (2021a). Stripping Torque Model for Bone Screws. *IFAC-PapersOnLine*, 54(15), 442–447. doi:10.1016/j.ifacol.2021.10.296.

Wilkie, J., Docherty, P.D., Stieglitz, T., and Möller, K. (2021b). Geometric Generalization of Self Tapping Screw Insertion Model. In *2021 43rd Annual International Conference of the IEEE Engineering in Medicine Biology Society (EMBC)*, 4387–4339. doi:10.1109/EMBC46164.2021.9630157.

Wilkie, J., Docherty, P.D., Stieglitz, T., and Möller, K. (2021c). Quantifying Accuracy of Self-Tapping Screw Models. In *2021 43rd Annual International Conference of the IEEE Engineering in Medicine Biology Society (EMBC)*, 4391–4394. doi:10.1109/EMBC46164.2021.9630646.

Wilkie, J., Rauter, G., and Möller, K. (2023). Initial validation of automatic torque-limiting bone screwdriver system. *Proceedings on Automation in Medical Engineering*, 2(1), 759–759.

Wright, B.J., Grigg, S., Bergsaker, A.S., Brattgjerd, J.E., Steen, H., and Pullin, R. (2020). Real time monitoring of screw insertion using acoustic emission can predict screw stripping in human cancellous bone. *Clinical Biomechanics*, 76, 105026. doi:10.1016/j.clinbiomech.2020.105026.